

Prediction of Transition on Wings in a RANS Approach

C. de Nicola¹, L. Graziosi¹, R. S. Donelli³

¹*Dipartimento di Ingegneria Aerospaziale, Università Federico II - P.le Tecchio 80125, Napoli*
E-mail: denicola@unina.it, lucagraziosi@libero.it

²*CIRA, Italian Center for Aerospace Research - Via Maiorise, Capua (CE), 81043, Italy*
E-mail: r.donelli@cira.it

Keywords: Aerodynamics, Transition Prediction, Boundary Layer, CFD

SUMMARY. A numerical procedure to improve the performances of a RANS code by including an accurate prediction of the location of the transition onset is presented. Application have been limited to wings. The final objective is to overcome the inaccuracy of RANS in predicting the transition from laminar to turbulent flow.

1 INTRODUCTION

Transition is now understood to be an important phenomenon even in the prediction of largely turbulent flows, since it has a major influence on friction drag, leading edge separation and boundary layer thickness, the latter impacting upon other key features such as shock-wave position and associated wave drag in transonic flows. A correct prediction of the high-speed drag coefficient of an airplane is crucial for a well founded design procedure. Otherwise the stall mechanisms could be captured only if the role of the transition is completely clarified: the achievement of a good agreement with experiment for high-lift flows is impossible without correct informations about the transition. Likewise, the extrapolation of wind tunnel results to flight scale by using CFD depends upon an accurate resolution of the transition phenomenon.

In the Authors experience, existing RANS approaches, [1], suffer of inadequateness in the capability of the turbulence models to predict the transition with the accuracy required for aeronautical applications in cruise and high-lift conditions. In general, credible laminar-turbulent simulations can be performed only if the transition location has been fixed.

The achievement of a reliable transition modeling capability in Navier-Stokes solvers will therefore give a significant contribution to the efficiency of the industrial aerodynamic design process, as well as increasing confidence in the design products.

In this work a numerical procedure to improve the performances of a RANS code by including an accurate prediction of the location of the transition onset is proposed. The present application has been limited to wings. The final objective is to overcome the inaccuracy of the turbulence models in predicting the transition from laminar to turbulent flow.

2 TRANSITION MECHANISMS ON A WING

At least three main mechanisms govern transition phenomena on swept wings, that have been summarized in Figure 1, [2].

First, the attachment line contamination. This phenomenon occurs when turbulence convected along the fuselage propagates along the swept leading edge and then contaminates the wing surface. This kind of instability is strongly affected by the leading edge wing radius, as observed by Pfenninger during the laminar flow control flight tests with the X21 aircraft [3]. He formulated a criterion, later perfected by Poll [4], based on the attachment line Reynolds number $\bar{R} < 245$, where

\bar{R} is defined as $\frac{We}{\sqrt{\nu \bar{U}_e}}$, We is the spanwise velocity component along the attachment line, \bar{U}_e is the chordwise pressure gradient and ν is the kinematic viscosity. For compressible flows, a modified Reynolds number \bar{R}^* is obtained from \bar{R} by applying an empirical compressibility function [5] and used in the same criterion. The criterion allows to predict attachment line contamination for a given sweep and curvature of the leading edge.

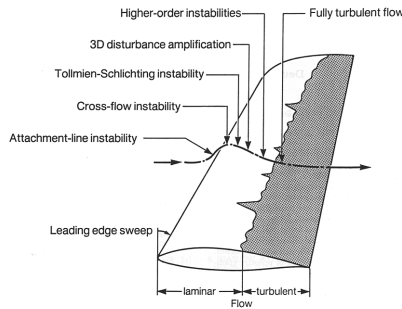


Figure 1: Transition phenomena on a swept wing.

The other two mechanisms have a common origin. According to Morkovin [6, 7], close to the leading edge, in a region known as the “receptivity region”, the external disturbances, such as free stream turbulence, engine noise, acoustic waves, enter the boundary layer and generate unstable waves. These disturbances, even if the frequency is the same of the boundary layer instabilities, have wavelengths much longer. So, resonance between boundary layer instabilities and exciting waves take place only thanks to the receptivity mechanism that adapts the disturbances wavelengths to the resonant ones. This is obtained through the effect of the boundary layer growing in the neighborhood of the leading edge or because of the fast adaptation of the boundary layer due to the wall roughness, wall waviness, blowing/suction and so on.

The second and third mechanisms that trigger transition are the Tollmien-Schlichting (TS) and crossflow (CF) waves amplification. In a first phase, through the receptivity, forced disturbances (free-stream turbulence, free-stream noise, vibrations, small roughness elements) enter the laminar boundary layer and excite its eigenmodes. In a second phase, these eigenmodes take the form of periodic waves, which energy is convected in the downstream direction. Some of them are amplified and will be responsible for transition. Their evolution is fairly well described by the linear stability theory [8, 9], as well as from some specific criteria. When the wave amplitude becomes finite, nonlinear interactions occur and lead rapidly to turbulence. Hence, on a swept wing, distinction is made between two types of linearly growing waves: the Tollmien-Schlichting (TS) waves and the crossflow (CF) waves. TS waves are the result of the instability of the streamwise mean velocity profile, i.e. the component of the mean velocity profile in the external streamline direction. These waves are unstable in regions of zero or positive pressure gradients. CF waves are the result of an instability of the mean crossflow velocity profile (the crossflow is the velocity component normal to the streamwise direction). These waves are unstable in regions of negative pressure gradient, typically in the vicinity of the leading edge where the flow is strongly accelerated.

3 LINEAR STABILITY THEORY AND ENGINEERING CRITERIA FOR TRANSITION

The present work deals with the hypothesis of a linear evolution of the boundary layer disturbances. In this context, several approaches can be followed to individuate transition depending on accuracy and time demanding of the solution: a short description follows.

3.1 Linear Stability Analysis and e^N method

The most common transition prediction method is the e^N method [10], based on the relative amplification of the discrete frequency disturbance which first reaches a preset “transition level” of e^N . It involves the stability analysis of a laminar boundary layer by solving the linear equations of the non-stationary disturbances superposed to the basic motion. Assuming a quasi-parallel flow, the compressible linearized Navier-Stokes equations admit a normal mode solution in the form of a harmonic wave

$$\varphi(\bar{x}, \bar{y}, \bar{z}, t) = A(\bar{y})e^{i(\alpha\bar{x} + \beta\bar{z} - \omega t)} \quad (1)$$

where φ is a velocity, pressure or density fluctuation, $A(\bar{y})$ is the amplitude function, \bar{x} and \bar{z} are the direction normal and parallel to the leading edge and \bar{y} is the direction normal to the wall. The introduction of expression (1) in the linearized Navier-Stokes equations leads to a system of ordinary differential equations: these equations and the related boundary conditions are homogenous and represent an eigenvalue problem that admits a non-trivial solution only when the dispersion relation $\omega = \omega(\alpha, \beta)$ is satisfied [8]. Usually, the problem is solved by following two different theories:

- a spatial theory, where α and β are assumed to be complex and ω real;
- a temporal theory, where α and β are assumed to be real and ω complex.

The solution of the linear system of equations allows to determine the growth rate of the disturbances. The N factor represents the amplitude ratio for each frequency obtained by integrating the spatial amplification rate as follows (σ is the imaginary part of the disturbance growth rate):

$$N = \log \left(\frac{A}{A_0} \right) = \int_{x_0}^x -\sigma(x) dx \quad (2)$$

3.2 Engineering Criteria for T-S

A large investigation of the Falkner-Skan laminar self-similarity solutions by using the e^N method coupled to the linear stability theory was performed by Arnal to improve the Granville criterion to predict the onset of transition of Tollmien-Schlichting waves. This criterion accounts for stability properties and flow history. The stability is characterized by the difference between the values of the Reynolds number based on the momentum thickness at the transition and at the neutral stability points, namely $R_{\theta_T} - R_{\theta_{cr}}$, while the flow history is characterized by an averaged Pohlhausen parameter

$$\bar{\Lambda}_2 = \frac{1}{X_T - X_{cr}} \int_{X_{cr}}^{X_T} \frac{\theta^2}{\nu} \frac{dU_e}{dx} dx \quad (3)$$

The location X_T of the transition onset is individuated when R_θ becomes equal to the value R_{θ_T} provided by

$$R_{\theta_T} - R_{\theta_{ins}} = -206e^{(25.7\bar{\Lambda}_2)} (\ln 16.8Tu - 2.77\bar{\Lambda}_2) \quad (4)$$

where Tu is the turbulence intensity of the external flow. The values of x_{ins} and $R_{\theta_{ins}}$ are determined when the Reynolds number R_θ computed in laminar flow becomes equal to the $R_{\theta_{cr}}$. It is assumed that $R_{\theta_{cr}}$ is a function of the shape factor H with:

$$R_{\theta_{cr}} = \left[\frac{e^{5.27+17.2[\frac{1}{H}-0.39]^{0.5}}}{H} \right] \quad \text{for } H < 2.5 \quad (5)$$

$$R_{\theta_{cr}} = \left[\frac{e^{3.5+\frac{2.897}{H}+\frac{22230}{H^{10}}}}{H} \right] \quad \text{for } H > 2.5 \quad (6)$$

The free stream turbulence is assumed appearing either by streamwise instability or by cross-flow instability, so the criteria are applied separately for each one of these mechanisms, and it is assumed that the boundary layer will cease to be laminar as soon as one of them is satisfied. In a three-dimensional flow the "natural" transition can occur from the same type of instability as in two-dimensional flow, so it can be predicted by applying simple two-dimensional criteria along the external streamline.

3.3 Engineering Criteria for Crossflow

The transition can be caused by crossflow instabilities that, as before described, develop in regions where the streamwise waves are stable (favorable pressure gradient regions). On swept wings transition dominated by crossflow can occur very close to the leading edge even if streamwise velocity profiles are stable.

One of the most famous crossflow instability criteria to predict the onset transition is the so-called C_1 [11], an experimental correlation between two boundary layer integral parameters at the transition location, the crossflow Reynolds number and the streamwise shape factor H:

$$(R_{\delta_2})_T = \frac{300}{\pi} \arctan \left[\frac{0.106}{(H - 2.3)^{2.052}} \right] \quad 2.3 < H < 2.7 \quad (7)$$

The crossflow Reynolds number is defined as

$$R_{\delta_2} = \frac{1}{\nu} \int_0^{\delta} w dy \quad (8)$$

3.4 Leading Edge Contamination

The leading-edge contamination is a phenomenon that has to be taken into account in the design, as well as in the estimation of the aerodynamics performances of a swept laminar wing. It depends from the turbulent boundary layer that develops on the fuselage and propagates along the attachment line of a swept leading edge in spanwise direction. When the turbulence spreads over the wing surface, the flow on the swept wing can be considered fully turbulent. A criterion to establish the state of the flow on the swept wing is based on the parameter \bar{R}^* defined as

$$\bar{R}^* = \frac{W}{\mu} \cdot \sqrt{\left(\frac{\mu}{k}\right)} \quad (9)$$

where W is the velocity component parallel to the leading edge, μ is the local kinematic viscosity, k is the gradient of velocity normal to the leading edge along this normal direction. When $\bar{R}^* < 245$ the leading edge is laminar, otherwise it is turbulent.

4 BOUNDARY LAYER TRANSITION CRITERIA INTO A RANS SOLVER

The calculation of a RANS solution for which the transition is evaluated by means of transition criteria well assessed for boundary layer flows is the basic idea of the work. The boundary layer calculated in the RANS procedure is not considered: the starting point is that the RANS surface pressure distribution is the same pressure distribution at the outer edge of the boundary layer.

Really, one of the difficulties in implementing local transition boundary layer criteria in a RANS solver is that in a RANS flow field the boundary layer cannot be easily defined and separated from the remaining (the 'external' flow field), even if methods for properly individuate the boundary layer in a RANS flow field have been proposed for some applications, [12].

So in this method the (iterative) RANS calculation around an airplane is cyclically stopped and the actual laminar boundary layer characteristics and the transition onset regions are re-evaluated by using a boundary layer method starting from the RANS actual external pressure distribution: so this step is autonomous from the RANS computation, that is temporary idle. Then the transition location is updated for the RANS calculation, that restarts. By iterating this scheme a converged RANS solution can be achieved with a proper prediction of the transition. More in detail:

- at fixed iterations the RANS calculation is temporary stopped, the partially converged wing surface pressure distributions are extracted and used as input to the boundary layer solver;
- velocity and temperature boundary layer profiles are computed and used, in order to identify the transition onset for the upper and lower wing surface;
- then these predicted locations of the transition onset are transferred into geometrical and topological information to be provided back to the RANS code
- then the RANS calculation starts again;
- this coupling procedure among RANS and boundary layer solvers and transition criteria is iterated until some convergence requirements -starting from the invariance of the location of the transition, and enclosing convergence criteria on residuals and force coefficients- have been satisfied.

The resulting flow field has the properties of a RANS solutions with a proper and robust treatment of the transition. It is obvious that this method is advantageous in the case of free transition, or when the transition is assigned downstream with respect to a reasonable location, i.e. past the body.

4.1 *Present Application*

The present interest is directed toward realistic calculations around airplanes: as a consequence, in the present procedure a fully turbulent RANS calculation has to be set, and the proper value for the free stream turbulence boundary condition is to be assigned.

It is to be noted that in this way RANS will predict a 'laminar' boundary layer that has to be intended as a region with very low (practically, zero) turbulence intensity: in that region the asymptotic turbulence (and any other disturbance) is destroyed by the viscous stresses. When the turbulence produced into the boundary layer by the turbulence model grows up, the 'turbulent' boundary layer begins.

It is to be confirmed that these RANS boundary layer characteristics are ignored in the successive explicit boundary layer and laminar instability points calculation: only when convergence on the location of these points have been reached, the final RANS solution can be considered as correct (in the boundary layer also) and used in order to compute forces and moments.

The RANS flow solver used for the numerical simulations is the FLUENT commercial code. It solves the Reynolds Averaged Navier-Stokes equations on unstructured hybrid grids by means of the Finite Volume method: anywhere, present applications have to be performed on structured grids (that FLUENT consider as intrinsically unstructured). This is due to the requirements imposed by the boundary layer solver concerning the mesh over the surface, that should be structured.

A second order upwind scheme was adopted for the spatial discretization, whereas a compressible formulation was chosen as governing mathematical model. The pressure-velocity coupling was ensured by means of the SIMPLEC algorithm and by using a pressure-staggering approach. Moreover, the isothermal flow assumption allowed the energy equation to be disregarded. The so called segregated implicit solution procedure was used, where each single flow equation is solved sequentially. Turbulence models used in the numerical simulations are the Spalart-Allmaras (S-A) model, the $k-\epsilon$ Realizable model and the $k-\epsilon$ RNG model. For both the $k-\epsilon$ models utilized the Enhanced Wall Treatment option was activated in order to include wall effects in a low-Reynolds-number turbulence modeling fashion. Details on the flow solver characteristics can be found in [13].

The (laminar) boundary layer method that has been used is well suited for straight and swept tapered wings, [14]. The boundary layer equations are rewritten in a conical reference frame and solved along the intersection of a sphere with the upper and lower wing surfaces, Figure 2. The transition criteria have been previously introduced and described.

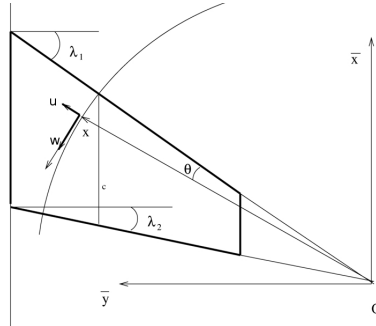


Figure 2: Conical reference frame for the boundary layer solver

Interface modules able to manage in a automatic way the I/O of both FLUENT and the boundary layer solver have been developed, [15]. The pressure distribution can be extracted directly from the actual RANS solution for boundary layer and laminar instability calculation. In order to properly reset the laminar region for the RANS solver, a software based on the so called User Defined Function (UDF) of FLUENT, a powerful tool, has been written.

The procedure, Figure 3, has been automatized, and can run in batch mode.

5 NUMERICAL RESULTS FOR THE NLF-0414F AIRFOIL

The validation of this procedure requires significative test cases for which experimental reliable data are available both in terms of pressure distributions and of measured transition locations. The test case individuated for a preliminary 2D application is the low-speed Natural Laminar Flow airfoil NLF-0414F, designed at NASA Langley following the primary objective of achieving significantly lower profile drag coefficients at cruise than existing NLF airfoils, but practical to use. This resulted in an exercise to design an airfoil with an extensive pressure favorable gradients ($dp/dx < 0$)

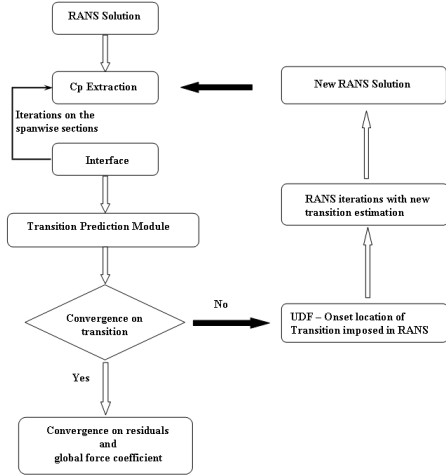


Figure 3: Flowchart of the procedure to include the onset transition in RANS.

but avoiding too severe far aft pressure recoveries. The airfoil was designed for reasonably high Reynolds numbers, approximately 10^7 , and tested for several wind tunnel flow conditions [16]. The present procedure has been applied in the design flow condition reported below.

Design Flow condition		
Mach	C_l	Rey
0.4	0.461	10^7

A single block grid with a C topology has been used in the computations. The number of points is 769 in the chord-wise direction and 96 in the normal direction. The number of points on the airfoil surface is 575. The RANS computation has been performed using the Spalart Allmaras turbulence model. The flow field has been initialized in fully turbulent mode.

Each 2000 iterations, the procedure delivers a pressure distribution to the transition prediction module which estimates the onset of transition for the upper and lower surfaces. The obtained values are then translated into geometrical and topological information to be provided back to the RANS code. Hence, the simulation starts again. The transition prediction procedure stops when the invariance on the transition location is found in the iterative process, i.e. when transition location change falls within 1% chord. After that, the CFD run is continued until classical CFD convergence criteria on variable residuals and global force coefficients are satisfied.

Upper and Lower onset location of transition	
$(x/c)_{TR_{upper}}$	$(x/c)_{TR_{lower}}$
0.5386	0.6336

Figure 4 shows the convergence history of the onset of transition for the upper (on the left) and lower (on the right) surface. The run was started with the option "fully turbulent" and after the first iteration the onset of transition was found and imposed at about 57% and 62.5% of the chord, for upper and lower surface, respectively. After the first iteration the onset of transition moves

downstream on both surfaces. Six iteration processes are sufficient to individuate the final onset location of transition.

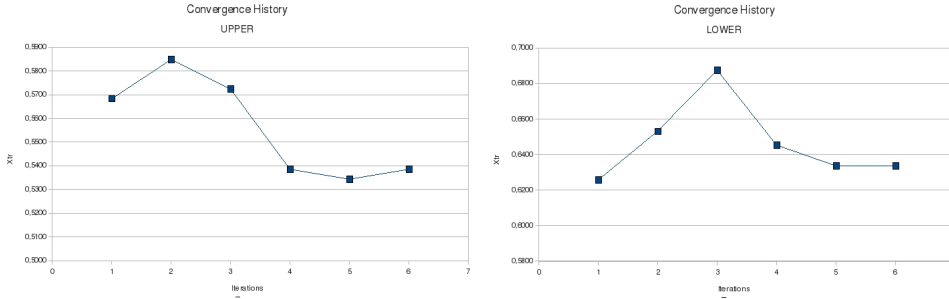


Figure 4: Convergence history of the onset of transition - Upper (left) and Lower (right) surfaces .

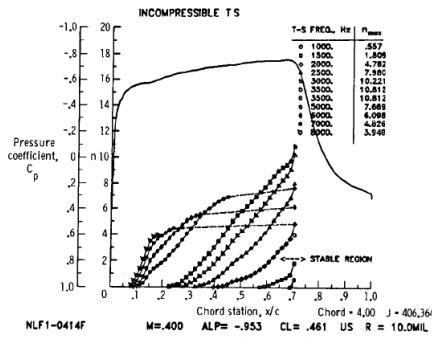


Figure 5: Linear stability analysis and N factor curves.

The experimental measurements indicated a transition location at 70% of the chord. This was confirmed from the stability analysis performed by NASA Langley and showed in Figure 5. The N factor curves reach the typical N factor values of 9-10 at about 0.7 of the chord, where the flow becomes fully turbulent. These results are not in contrast with the present ones. Figure 6 shows the upper and lower skin friction coefficient computed in the present application. As can be observed, the skin friction coefficient presents a sudden change in proximity of the 70% of the chord pointing out the passage from laminar to turbulent flow.

Figure 7 (left side) shows the satisfactory comparison of the pressure distribution (present computation vs. experiments), even if some small discrepancies exist in the expansion region of the upper surface.

In Figure 7 (right side) the comparison between the pressure distributions computed in fully turbulent conditions and from the procedure has been reported: the difference is not negligible. Drag and lift coefficients reported in the table below for these two flow conditions clearly point out the importance of accurately predict transition from laminar to turbulent flow. By neglecting transition the lift coefficient is underestimated (about 10%) while the drag coefficient is increased twofold: the

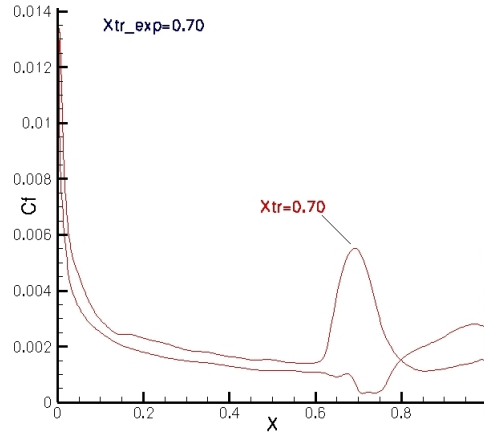


Figure 6: Skin friction coefficient on the upper and lower surface.

aerodynamic performances are strongly affected by transition phenomena and, as a consequence, it becomes extremely important to introduce accurately a model for transition in RANS approaches.

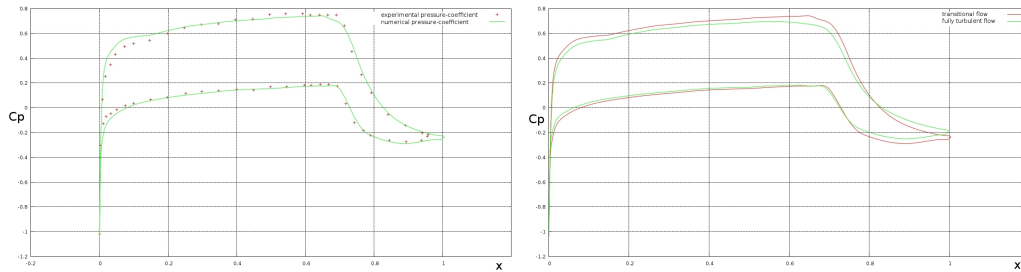


Figure 7: Pressure distributions: (Left) Computed vs Experiments - (Right) Computed Transitional vs. Computed Fully Turbulent

Lift and drag coefficient for transitional and turbulent flow	
$C_{l_{trans.}} = 0.4603$	$C_{l_{turb.}} = 0.4216$
$C_{d_{trans.}} = 6.44 \times 10^{-3}$	$C_{d_{turb.}} = 1.29 \times 10^{-2}$

6 CONCLUSIONS

The main objective of this work has been the development of a tool to predict the transition location in a RANS solver, that is an issue still open. An algorithm to prescribe the transition in a topology-independent way has been developed and validated, but only for 2D flows. However further investigations for other test cases, like multi-component airfoils, are needed. The present algorithm has been developed for 3D flows, and the validation is in progress: the M6 ONERA swept wing has been selected as the first test case in order to evaluate the effectiveness of the procedure in the prediction of transition caused by leading edge contamination and crossflow waves.

References

- [1] Menter, F.R., Langtry, R., Volker, S. and Huang, P.G., “Transition Modelling for General Purpose CFD”, *ERCOFTAC Int. Simp. on Engineering Turbulent Modelling and Measurements*, ETMM6, 2005.
- [2] Schrauf, G., Bieler, H. and Thiede, P., “Transition Prediction - the Deutsche Airbus View”, *First European Forum on Laminar Flow Technology*, DGLR, AAAF, RAeS, Hamburg, Germany, March 16-18 1992.
- [3] Pfenninger, W., “Laminar Flow Control-Laminarization”, *AGARD, Tech. Rep. 654*, June 1977.
- [4] Poll, D.I.A., “Transition in the Infinite Swept Attachment Line Boundary Layer”, *Aeronautical Quarterly*, Vol. 30, 1979, pp. 607–628.
- [5] Poll, D.I.A., “Boundary Layer Transition on the Windward Face of Space Shuttle During Reentry”, *AIAA P.*, No. 85-0899, 1985.
- [6] Morkovin, M., “Instability, Transition to Turbulence and Predicability”, *AGARD T.R. 236*, July 1978.
- [7] Morkovin, M., “Recent Insights into Instability and Transition to Turbulence in Open-Flow Systems”, *AIAA J.*, Vol. 88-3675, 1988.
- [8] Mack, L.M., “Boundary Layer Linear Stability Theory”, *Proc. Special Course on Stability and Transition of Laminar Flows 709*, AGARD, VKI, Brussels, 1984.
- [9] Mack, L.M., “On the Stability of the Boundary Layer on a Transonic Swept Wing”, *AIAA J.*, Vol. 79-0264, 1979.
- [10] Arnal, D., “Boundary Layer Transition: Predictions Based on Linear Theory”, *AGARD T.R. 793*, 1994.
- [11] Arnal, D., “Computation of Three-Dimensional Boundary Layers Including Separation”, *AGARD T.R. 741*, 1986.
- [12] Papparone, L. and Tognaccini, R., “Computational Fluid Dynamics-Based Drag Prediction and decomposition”, *AIAA J.*, Vol. 41, No. 9, Sept. 2003, pp.1647-1657
- [13] Fluent 6.1, Users Guide, February 2003
- [14] Kaups, K. and Cebeci, T., “Compressible Laminar Boundary Layer with Suction on swept and tapered wings”, McDonnell-Douglas Corporation, MDC Report J7337, 1976
- [15] Graziosi, L., de Nicola, C. and Donelli, R.S., “Integrazione in Codici RANS di una Procedura per la Stima della Transizione”, DIAS Report (in Italian), University of Naples, dec. 2009
- [16] Viken, J.K., Viken, S.A., Pfenninger, W., Morgan, H.L. and Campbell, R.L., “Design of the Low-Speed NLF-0414F and the High-Speed HSNLF-0213 Airfoils with High-Lift Systems”, NASA Langley Research Center Report N90-12540